THE REDUCTION OF CHROMITE SPINELS BY SOLID CARBON AND CARBON DISSOLVED IN LIQUID ALLOYS

R H ERIC, O SOYKAN & E USLU

Department of Metallurgy
and Materials Engineering
University of the Witwatersrand

ABSTRACT

The reduction behaviour of chrome spinels from the Bushveld Complex has been studied by a number of techniques, including thermogravimetric analysis (TGA), the rotating-cylinder technique (RCT), X-ray-diffraction analysis (XRD), energy-dispersive analysis by X-rays (EDAX), electron-microprobe analysis (EMPA), and metallography.

In solid-state reduction work at temperatures between 1300 and 1450°C, TGA showed that the reduction rate increases with increasing temperature, decreasing particle size, and decreasing Cr_2O_3 content and chromium-to-iron ratio in the ore. Zoning in partially reduced chromites was observed metallographically. EDAX revealed that the inner core was rich in iron, while the outer core was depleted in this species. EDAX examination also showed outward diffusion of Fe^{2+} and Cr^{3+} ions and inward diffusion of Cr^{2+}, Al^{3+}, and Mg^{2+} ions. A reaction mechanism for reduction based on the findings was developed. The mechanism is mineralogical in nature, and assumes that the stoichiometry of the spinel phase remains constant as the reduction increases. The mechanism is also unique in that Cr^{2+} ions are present, which reduce the Fe^{3+} ions under the surface of the particle to the Fe^{2+} state at the interface between the inner and outer cores.

The reduction of solid chromite by carbon dissolved in liquid ferrochromium alloys was studied in the temperature range 1500 to 1680°C by the RCT. The decarburization of the metal (and hence the reduction of the chromite), increased with increasing temperature, carbon content of the bath and rotational speed up to about 400 r/min, after which it remained constant. In the later stages of the reduction, carbides of high liquidus temperature, mainly $(Fe, Cr)_7C_3$, formed round the chromite cylinder. This layer hindered direct contact between the chromite and the liquid metal. Further reduction occurred either by the diffusion of carbon through this carbide layer to the carbide-oxide interface, or by the diffusion of carbon monoxide gas through microcracks.

INTRODUCTION

Chromite ores comprise chrome spinels combined with physically separable gangue minerals. The chemical formula of chrome spinels can be represented as AB_2O_4, where A represents divalent cations (i.e. Fe, Mg) in the tetrahedral sites, and B represents trivalent cations (i.e. Cr, Al, Fe) in the octahedral sites. In some cases, tetravalent cations (i.e. Ti) replace trivalent cations in the octahedral sites, making an ulvospinel, i.e. Fe_2TiO_4, in which half of the divalent iron ions occupy tetrahedral sites, while the others occupy octahedral sites. Each unit cell is made up of eight AB_2O_4 units, where the cubic close-packing of 32 oxygen atoms provides 64 tetrahedral and 32 octahedral sites.[1]

Normal spinels have eight divalent cations in the tetrahedral sites and 16 trivalent cations in the octahedral sites, e.g. $Fe^{2+}(Cr^{3+})_2O_4$. Inverse spinels have eight of the 16 trivalent cations in tetrahedral sites; the octahedral sites are occupied by eight trivalent and eight divalent cations, e.g. magnetite, $Fe^{3+}(Fe^{2+},Fe^{3+})O_4$. There are many spinels in which the distribution of cations lies between these two extremes.[2,3]

The reduction of any crystal requires the migration of atoms or ions, which is possible if imperfections exist.[4] In chrome spinel, the sub-lattice of the oxygen ion is almost perfect compared to that of the cation. This can be concluded from the almost complete dense packing and the relatively large radius of the oxygen ion. It is also known that the oxygen-diffusion coefficients[5,6] are several orders of magnitude smaller than the cation-diffusion coefficients. Therefore, during the initial stages of reduction, the removal of oxygen atoms from the surface of a chromite particle is accomplished by the electrically balanced reduction of Fe^{3+} to Fe^{2+} by the reductant. Further reduction will continue at the surface by the reduction of Fe^{2+} ions to the metallic state. This results in the creation of an Fe^{2+} concentration gradient between the surface and the interior of the particle, which causes the Fe^{2+} ions to diffuse out of the particle, leaving a cation vacancy in the unit cell. Because of the removal of Fe^{2+} ions, the ratio of divalent to trivalent cations in the unit cell beneath the surface decreases. Hence, the spinel becomes saturated with trivalent oxides, and the removal of iron from the system can be regarded as being equivalent to the addition of the trivalent cations Cr^{3+}, Al^{3+}, and Fe^{3+} to the spinel. This is, in fact, the same as the dissolution of the defect spinels, γ-Al_2O_3, γ-Cr_2O_3, and γ-Fe_2O_3 in the stoichiometric spinel. Since Fe^{3+} is unlikely to be present under highly reducing conditions, only γ-Al_2O_3 and γ-Cr_2O_3 can be expected to contribute to the non-stoichiometry in the spinel. Equilibrium constants for vacancy concentrations have been established only in the spinel end-member Fe_3O_4.[7] However, no experimental information

is currently available concerning the distribution and concentration of vacancies in mixed spinels, and the relationship between cation vacancies and temperature-dependent departures from stoichiometry is not clear, and has not been investigated.

Because of the lack of data on defect concentrations and cation distributions in mixed spinels, the solid-state reduction mechanism of chrome spinels at around 1400°C could not be based on imperfections. The interpretation of data gathered from X-ray diffraction analysis (XRD) and energy-dispersive analysis of X-rays (EDAX) was therefore based on the stoichiometry of the spinel phase. Stoichiometry was assumed to hold good with increasing reduction during which part of the Cr^{3+} ions were reduced to Cr^{2+}. The proposal that Cr^{2+} ions were present in the spinel was based on the observation of Ulmer and White[1] who detected small concentrations of divalent chromium ions in spinels in the $FeCr_2O_4$-$MgCr_2O_4$ solid-solution series equilibrated with iron at 1300°C. In the present model, the existence of an ordered spinel structure was assumed with Cr^{2+} in tetrahedral sites (when necessary) together with Mg^{2+} and Fe^{2+}. The calculations were based on the ideal structural formula, i.e. a ratio of the divalent cation to trivalent cation to anion of 1:2:4. The amount of oxygen combined with the spinel structure was determined by the neutrality of the charge.

The reduction of chrome spinels at temperatures between 1500 and 1680°C by carbon dissolved in liquid ferrochromium alloys has a direct bearing on the refining of high-carbon ferrochromium alloys and the direct production of stainless steel from chromium- and iron-containing ores. Hence, the available oxygen, in the form of iron and chromium oxides, can be employed as an oxidant for carbon in addition to gaseous oxygen.

The reduction behaviour of chrome spinel by carbon dissolved in high-carbon ferrochromium alloys was studied, by use of the following reaction

$$FeCr_2O_4(s) + 4\underline{C} = Fe(\ell) + 2Cr((\ell) + 4CO(g). \quad (1)$$

Sintered cylinders of chrome spinel were immersed in a bath of ferrochromium alloy, and rotated at different speeds. The reaction rate was analysed in terms of the decarburization of the melt. Partially reacted chromite samples were subjected to metallographic examination, EDAX, XRD, and electron-microprobe analysis (EMP) so that the mechanism of reduction could be determined. A multistage reaction mechanism for the reduction of natural chromite at 1600°C by carbon dissolved in liquid ferrochromium alloy was proposed. The most noteworthy aspect of the mechanism is the change from liquid-phase mass-transfer conditions in the earlier stages of the reaction to a solid-state reduction mechanism. This occurred because the chromite cylinders were covered with a layer of carbide that hindered direct contact of the molten alloy with the oxide. This phenomenon eventually brings the system into artificial equilibrium and as a result, the reaction virtually stops.

EXPERIMENTAL PROCEDURE

The chromite ore used in this study was from the LG-6 (lower group sixth seam) layer of the Bushveld Complex. The composition of the chromite, and the moles of cations per thirty-two oxygens, is given in Table I

TABLE I. Composition of the chromite ore as determined by chemical analysis

Component	Mass, %	Cation	Cation; Mol/ 32 Oxygens
Cr_2O_3	47.50	Cr^{3+}	9.728
Total Fe as FeO	26.25		
FeO	18.78	Fe^{2+}	4.079
Fe_2O_3 by difference	8.29	Fe^{3+}	1.569
Al_2O_3	14.90	Al^{3+}	4.707
MgO	9.70	Mg^{2+}	3.765
TiO_2	0.43	Ti^{4+}	0.078
CaO	0.05		
SiO_2	0.37		

Solid-state Reduction

Tests on solid-state reduction were conducted in the temperature range 1300 to 1450°C under inert argon-gas atmosphere. Fine powdered spectroscopic graphite was the reductant, and 30 per cent in excess of the stoichiometric requirement was used to reduce the iron and chromium oxides to the carbide $(Fe,Cr)_7C_3$. The loss in mass was measured continuously for each sample by a TGA facility attached to the bottom end of the furnace. The values for the loss in mass were then used in a determination of the percentage reduction by use of the following equation:

$$R, \% = \frac{\text{Mass of CO evolved}}{(28/16)\text{x (mass of original removable oxygen)}} \text{ x } 100. \quad (2)$$

After each reduction test, representative samples of the reaction products were split and prepared for XRD, EMPA and EDAX analyses. Point scans along a line in a particle were done by EDAX, and concentration profiles were constructed for chromium, iron, magnesium, aluminium, and titanium along selected cross-sections. The application of these mineralogical techniques to the reduced products revealed the reduction mechanism. The mechanism was based on data gathered at 1416°C.

Reduction of Chromite in Liquid Fe-Cr-C Alloys

The rotating-cylinder technique (RCT) was used to reduce the chromite and, simultaneously, to decarburize the liquid Fe-Cr-C alloys. The RCT facility was assembled on an inductively heated fused-silica tube furnace. The LG-6 ore was pulverized and formed into dry cylinders of 15mm diameter and 23mm length by uniaxial pressing in a steel mould. This was followed by sintering in an argon-gas atmosphere at 1400°C for 3 hours.

XRD and chemical analysis, showed that the changes in composition after sintering were negligible. Care was also taken to obtain cylinders that were free from cracks.
No measurable change in mass could be observed after sintering. The chromite cylinders were rotated at controlled speeds about their long axes by a flexible drive system, which was connected to a variable-speed electric motor by a stainless-steel rod. The Fe-Cr-C alloy was prepared from reagent-grade iron and chromium powders and spectroscopic-grade graphite. These constituents were placed in an alumina crucible of 47mm inner diameter and 68mm length in the RCT facility. The experiments were conducted in a neutral argon-gas atmosphere, and the chromite cylinders were immersed to a depth of 20mm in the liquid alloy when the system comprising the RCT and the induction furnace reached a steady temperature. The course of the reaction was determined by measurment of the change in the composition of the liquid alloy in terms of the decarburization rate. Metallographic examination, XRD, EMPA, and SEM-EDAX techniques were employed on reacted chromite samples so that the mechanism of reaction could be determined.

RESULTS AND DISCUSSION

Solid-state Reduction Mechanism

XRD analysis of unreduced chromite samples showed that chromium was present in the mixed chrome spinels of picrochromite, $(Mg,Fe)[Cr,Al]_2O_4$, aluminium chromite, $FeO(Al,Cr)_2O_3$, and donathite, $(Fe,Mg)[Cr,Fe]_2O_4$. The phases detected from the diffraction patterns of the reduced products are shown in Table II.

Another finding by XRD was the presence of MgO as a separate phase at reductions higher than 90 per cent. MgO was found deposited as a white powder covering the surface of the charge, and as white feathers at the top of the crucible. This appearance strongly suggested the involvement of a vaporous transport mechanism in the formation of this product.[8]

Electromicrographs and line scans for the elements chromium, iron, aluminium, magnesium, and titanium were carried out on particles that had been reduced to the values quoted in Table II by means of the SEM-EDAX facility. Figure 1 shows a typical electronmicrograph of a particle reduced 38.14 per cent, and a graph of the variations in element concentration across the line AB along this particle.

TABLE II. Major phases detected by XRD analysis in LG-6 chromite samples with increasing reduction at 1416°C

Reduction %	Phase detected *
2.08	Starting chromite, carbon
7.56	Starting chromite, carbon, α-iron
18.54) 25.20)	Picrochromite, carbon, α-iron
27.48) 38.14) 44.96)	Picrochromite, carbon, Fe_7C_3, $(Cr,Fe)_7C_3$
60.86) 64.74) 71.67) 76.17) 80.84)	$Mg(Cr,Al)_2O_4$, carbon, Fe_7C_3, $(Cr,Fe)_7C_3$, picrochromite
91.38	$Mg(Al_{1.5},Cr_{0.5})O_4$, $MgAl_2O_4$ $(Cr,Fe)_7C_3$, Fe_7C_3, carbon
99.05	$MgAl_2O_4$, $(Cr,Fe)_7C_3$, carbon

* Listed in order of decreasing intensity of diffraction peaks.

All the rest of the analyses showed similar concentration profiles up to a reduction of 72 per cent. Two distinct zones, an inner zone rich in iron and an outer zone depleted in iron, were visible in the back-scattered images of the reduced particles.

The zoning in reduced chromite grains has been observed by other investigators.[9-11] The sharp interface across the inner and outer zones is reminiscent of the topochemical interface often observed during the reduction of single-metal oxides. Searle and Finn also reported the presence of a sesquioxide phase $(Cr,Al)_2O_3$ adjoining the surface of the particle at temperatures below 1250°C.[11] This phase did not appear at temperatures greater than 1300°C in the present work. The concentration profiles that were determined revealed an iron-concentration gradient along the outer zone that suggests an outward diffusion of iron. Furthermore, the composition of the inner zone remained constant with increasing reduction, its composition being almost identical to that of starting chromite. The inner zone was observed to decrease in size with increasing reduction. It disappeared after 72 per cent reduction, and the particle then started to exhibit high porosity. Almost all the iron was reduced by the time 72 per cent reduction was reached.

In the light of the experimental data and observations, plots were constructed of the number of cations per 32 oxygens versus position (using EDAX profiles) on the assumption that the stoichiometry of the spinel holds with increasing reduction. Figure 2 illustrates the plots for a particle reduced to 38.14 per cent.

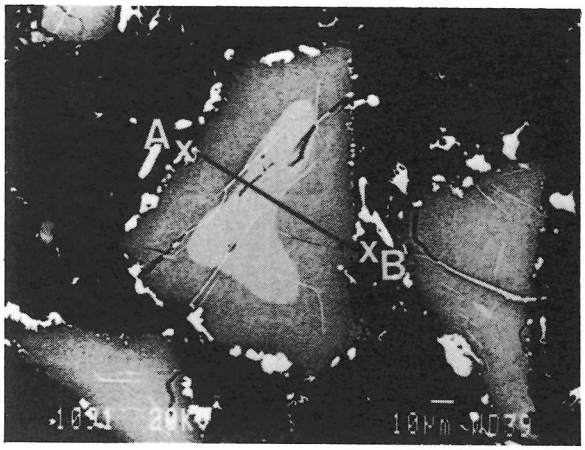

(a)

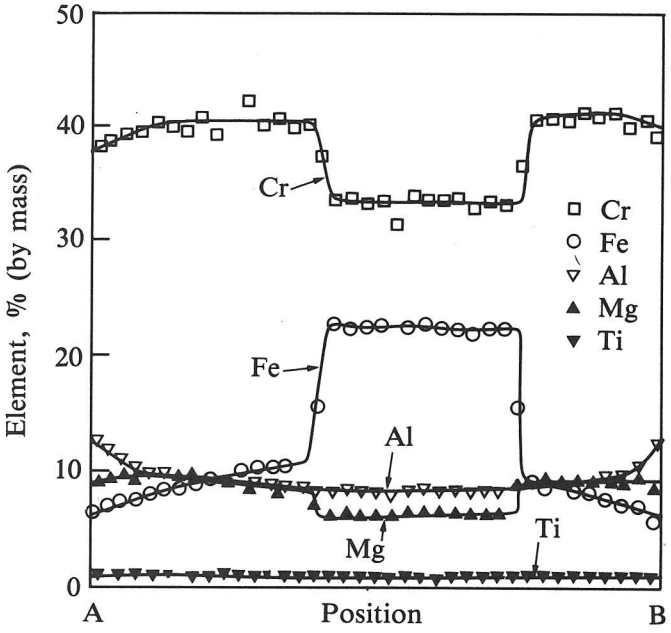

(b)

FIGURE 1. (a) Secondary electron image of an LG-6 chromite particle reduced to 38.14 per cent at 1416 °C;
(b) Variations in element concentrations across the line AB in (a)

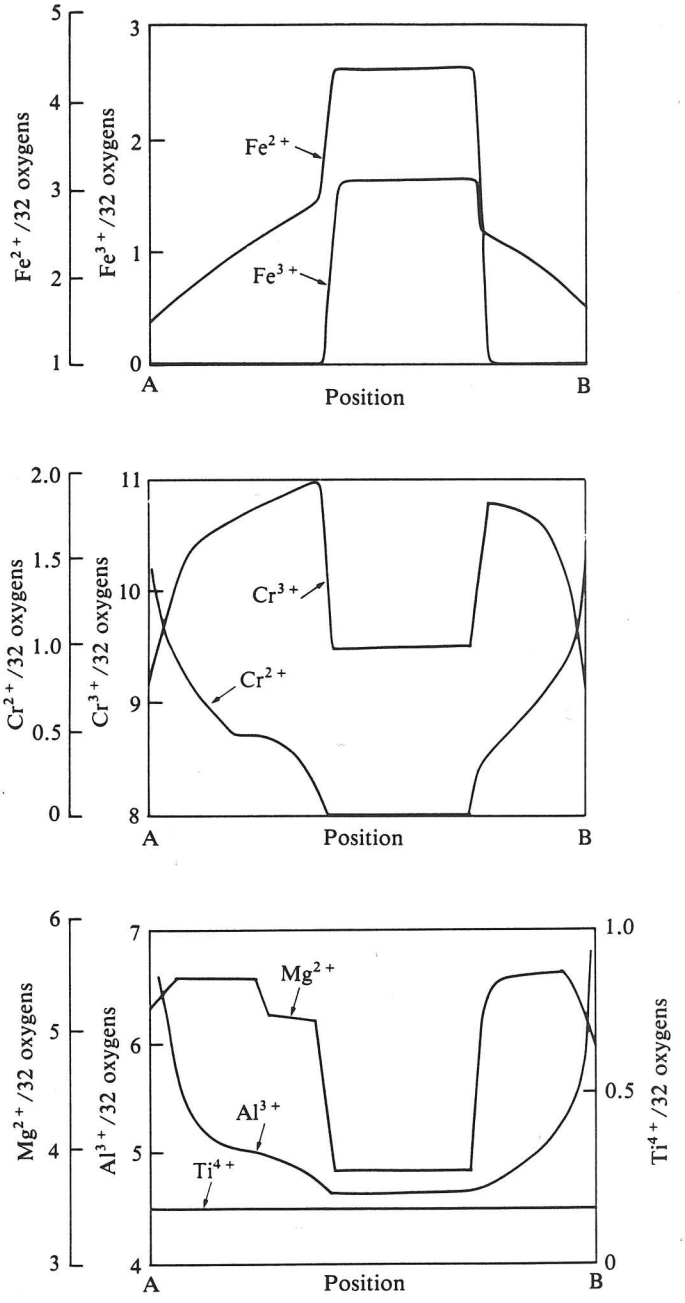

FIGURE 2. Variations in cations/32 oxygens across a particle that has undergone 38.14 per cent reduction

The moles of Fe^{3+}, Fe^{2+}, Cr^{3+}, Cr^{2+}, Mg^{2+}, Al^{3+} and Ti^{4+} that were calculated on the basis of the stoichiometric spinel model are not absolute values. The presence of Cr^{2+} ions was allowed up to a maximum of one Cr^{2+} per unit cell based on Creskovich and Shibican's study on tetragonal distortion in the spinel structure.[12] The concentration gradients of ions constructed in this manner, as shown in Figure 2, clearly showed that until the later stages of reduction Fe^{2+} and Cr^{3+} diffused to the surface and Cr^{2+} and Al^{3+} diffused towards the centre of the particle. Mg^{2+} ions showed a rather flat profile along the outer core, suggesting very fast inward movement as compared to the other species, as a result of which the particle shrank.

Although numerous studies have indicated that oxygen is a diffusing species, the diffusion of oxygen has not been substantiated in this study.[13,14] Charge neutrality was maintained by inward diffusion of Mg^{2+} and Al^{3+} ions. The reduction sequence was then based on the ionic concentration profiles and stoichiometry of the spinel phase discussed earlier. Furthermore, De Waal and Hiemstra, on the basis of the chemical analyses of ninety different chromite samples from the Bushveld Complex, found stoichiometry to a large extent.[15]

The formula for the unit cell of LG-6 chromite, based on values given in Table I, can be written as

$$(Fe_{4.08}Mg_{3.77})Cr_{9.73}Al_{4.71}Fe_{1.57}Ti_{0.08}]O_{32}. \quad (3)$$

On the other hand, if it is assumed that all the trivalent cations occupy 16 octahedral sites, that all the divalent cations are in the eight tetrahedral sites, and that Ti^{4+} makes ulvospinel, i.e. $(Me^{2+})[Me^{2+}Ti^{4+}]O_4$ (where Me^{2+} is Fe^{2+} or Mg^{2+}), the unit cell for LG-6 chromite can be represented by the following formula:

$$(Fe_{4.12}Mg_{3.88})[Cr_{9.63}Al_{4.66}Fe^{3+}_{1.55}Fe^{2+}_{0.08}Ti_{0.08}]$$
$$O_{32}, \quad (4)$$

where the parentheses and brackets refer to the tetrahedral and octahedral sites respectively. In the formula for LG-6 chromite(4), the valency of cations other than those referred to above have not been shown.

Each chromite particle is considered to be made up of concentric layers of unit cells, each of which has the composition shown in formula (4). The reduction of the unit cells situated on the surface of a chromite particle in contact with carbon and/or carbon monoxide gas is initiated by the reduction of Fe^{3+} ions to Fe^{2+} ions.

$$(Fe_{4.12}Mg_{3.88})[Cr_{9.63}Al_{4.66}Fe^{3+}_{1.55}Fe^{2+}_{0.08}Ti_{0.08}]$$
$$O_{32} + 0.775\ CO =$$
$$(Fe_{4.12}Mg_{3.88})[Cr_{9.63}Al_{4.66}Fe^{2+}_{1.55}Fe^{2+}_{0.08}Ti_{0.08}]$$
$$O_{31.225} + 0.775\ CO_2, \quad (5)$$

which is folowed by

$$0.775\ CO_2 + 0.775\ C = 1.55\ CO \quad (6)$$

The above reaction removes 0.775 oxygen ions from the unit cell, resulting in distortion. In order that the spinel structure can be retained, the reduction has to be accompanied by the removal of 2.325 mol of Fe^{2+} as metal.

$$(Fe_{4.12}Mg_{3.88})[Cr_{9.63}Al_{4.66}Fe^{2+}_{1.55}Fe^{2+}_{0.08}Ti_{0.08}]$$
$$O_{31.225} + 2.325\ CO =$$
$$(Fe_{3.345}Mg_{3.88})[Cr_{9.63}Al_{4.66}Fe^{2+}_{0.08}Ti_{0.08}]$$
$$O_{28.9} + 2.325Fe + 2.325\ CO_2. \quad (7)$$

The reduction proceeds by further distortion of the spinel structure until all the Fe^{2+} ions in the surface unit cell are reduced to metal, as follows

$$(Fe_{3.345}Mg_{3.88})[Cr_{9.63}Al_{4.66}Fe^{2+}_{0.08}Ti_{0.08}]$$
$$O_{28.9} + 3.425\ CO =$$
$$(Mg_{3.88})[Cr_{9.63}Al_{4.66}Ti_{0.08}]O_{25.475}$$
$$+ 3.425\ Fe + 3.425\ CO_2. \quad (8)$$

To build up the spinel structure in the surface unit cell, reaction (8) must be accompanied by the simultaneous reduction of Cr^{3+} ions, since Al^{3+} and Mg^{2+} have been accepted as being unreducible. The Cr^{3+} ions in the Mg-Cr-Al spinel at the surface are reduced to Cr^{2+} by the following reaction:

$$(Mg_{3.88})[Cr_{9.63}Al_{4.66}Ti_{0.08}]O_{25.475}$$
$$+ 1.135\ CO = 1.135\ CO_2 +$$
$$(Mg_{3.80}Cr^{2+}_{2.28})[Cr_{7.35}Al_{4.66}Mg_{0.08}Ti_{0.08}]$$
$$O_{24.34}. \quad (9)$$

Cr^{2+} ions, which diffuse inwards under a Cr^{2+} concentration gradient, will then reduce those Fe^{3+} ions in the unit cells just beneath the surface that are not accessible to the reductant, which are keeping the unaltered chromite composition. This is substantiated by the fact that, up to a reduction of 70 per cent, the particles are pore-free and dense. The reduction therefore proceeds under the surface via the following reaction:

$$(Fe_{4.12}Mg_{3.88})[Cr_{9.63}Al_{4.66}Fe^{3+}_{1.55}Fe^{2+}_{0.08}Ti_{0.08}]$$
$$O_{32} + 1.55\ Cr^{2+} =$$

$$(Fe_{4.12}Mg_{3.88})[Cr_{9.63}Al_{4.66}Fe^{2+}_{1.55}Fe^{2+}_{0.08}Ti_{0.08}]O_{32} + Cr^{3+}_{1.55}. \quad (10)$$

The Cr^{3+} ions have a very high preference energy for octahedral sites so they will exchange places with Fe^{2+} ions in the octahedral sites, which are very mobile compared to the ones in the tetrahedral sites.[16] In the meantime, Fe^{2+} ions diffuse out of the particle under an iron-concentration gradient, where they will be reduced to the metallic state. As the reduction proceeds, the replacement of 1.55 mol of Fe^{2+} by Cr^{3+} in the unit cells near the interface between the inner and outer cores will cause the unit cells just inside the outer core to be enriched in chromium and depleted in iron with respect to the unit cells just inside the inner core, which retain their original structure with increasing reduction.

For the further reduction of the Fe^{2+} ions in the unit cells beneath the surface unit cell, the Cr^{2+} ions of the surface unit cell must exchange places with the Fe^{2+} ions (in the tetrahedral sites) of the unit cells just below the surface.[1] The formula for the unit cell just under the surface is therefore now

$$(Fe^{2+}_{4.12}Mg_{3.88})[Cr_{11.18}Al_{4.66}Fe_{0.08}Ti_{0.08}]O_{32}, \quad (11)$$

and the formula for the surface unit cell is

$$(Mg_{3.80}Cr^{2+}_{2.28})[Cr_{7.35}Al_{4.66}Mg_{0.08}Ti_{0.08}]O_{24.34}. \quad (12)$$

After the Cr^{2+} ions of the surface unit cell have exchanged places with the Fe^{2+} ions of the unit cell just below, the formula will be

$$(Fe_{3.12}Mg_{3.88}Cr^{2+}_{1.0})[Cr_{11.18}Al_{4.66}Fe_{0.08}Ti_{0.08}]O_{32} \quad (13)$$

for the unit cell immediately beneath the surface, and the formula for the surface unit cell will be

$$(Mg_{3.80}Cr^{2+}_{1.28}Fe^{2+}_{1.0})[Cr_{7.35}Al_{4.66}Mg_{0.08}Ti_{0.08}]O_{24.34} \quad (14)$$

The reduction of Fe^{2+} at the surface will then proceed via the following reaction:

$$(Mg_{3.80}Cr^{2+}_{1.28}Fe^{2+}_{1.0})[Cr_{7.35}Al_{4.66}Mg_{0.08}Ti_{0.08}]O_{24.34} + 1.34\ CO = (Mg_{3.80}Cr^{2+}_{1.95})[Cr_{6.68}Al_{4.66}Mg_{0.08}Ti_{0.08}]O_{23} + Fe + 1.34\ CO_2. \quad (15)$$

Once the reduction of divalent iron is complete, the structure, as seen in reaction (15), comprises an Mg-Al-Cr spinel. The trivalent, and any divalent chromium ions present, are reduced to metal step by step by the reductant at the surface, while the stoichiometry of the spinel structure is retained, i.e.

$$(Mg_{3.80}Cr^{2+}_{1.95})[Cr_{6.68}Al_{4.66}Mg_{0.08}Ti_{0.08}]O_{23} + 1.32\ CO = (Mg_{3.80}Cr^{2+}_{1.62})[Cr_{6.02}Al_{4.66}Mg_{0.08}Ti_{0.08}]O_{21.68} + 0.99\ Cr + 1.32\ CO_2. \quad (16)$$

As the ratio of Al^{3+}-to-Cr^{3+} ions is larger in the surface unit cells, there will be an inward diffusion of Al^{3+} and an outward diffusion of Cr^{3+} ions. The final reduction product will be an Mg-Al spinel phase and MgO if the maximum solubility of MgO in the spinel phase is exceeded , i.e.

$$(Mg_{2.41})[Al_{4.66}Mg_{0.08}Ti_{0.08}]O_{9.64}. \quad (17)$$

In each of the stages described above, oxygen was removed from the surface. This mechanism is similar to that described for the reduction of iron ores.[17,18] It is obvious that the above mechanism, which is described stagewise, occurs simultaneously, and that metallized iron and chromium are present as their carbides, as determined by XRD of the reduced products.

Reduction of Chromite in Liquid Fe-Cr-C Alloys

Temperature, stirring, and the composition of the melt were the three main variables for the reduction of solid chromite in Fe-Cr-C alloys. These were tested as a function of time, and the results were analysed by the use of decarburization curves. The percentage decarburization is defined as

$$D, \% = [(C_i - C_f)/C_i] \times 100, \quad (18)$$

where C_i is the initial carbon concentration, and C_f is the final carbon concentration of the melt (as a percentage). It was established that 400 r/min was the optimum stirring rate, beyond which no appreciable improvement in the extent of decarburization was observed. This is unusual, but was also reported by Barmin et al. in their study of the rate of reduction of Cr_2O_3 disks by carbon in molten alloy.[19] They observed the same phenomenon at 570 r/min.

The effect of temperature was tested at the optimum stirring rate for 50% Cr - 6% C alloys at 1550, 1500 and 1680°C. As expected, decarburization, and hence the reduction of chromite, increased with temperature. The effect of the change in the chromium content of the melt was tested for alloys with carbon contents of 4, 5 and 7 per cent at 1500, 1600, and 1680°C. From the results of all these experiments, it was observed that irrespective of the temperature and carbon content of the

melt, decarburization increased with chromium content up to about 50 percent chromium in the alloy, and then decreased. The activity values taken from the literature for alloys with compositions similar to those used in the present work confirm that the ratios of the initial-to-final carbon activities increase with chromium content up to around 50 per cent chromium in the alloy, and then decrease.[20] For chromium-activity ratios, the situation is exactly the opposite. The behaviour of the activity ratios around 50 per cent chromium in the melt could explain the high decarburization at a chromium content of 50 per cent in the melt. This is illustrated in Figure 3.

It was also established that, for alloys with the same chromium content decarburization increased with increasing carbon content. However, the carbon content of the melt did not decrease to equilibrium values similar to those that would be expected thermodynamically. This suggested the presence of a barrier for the reduction reaction and, hence, an artificial equilibrium. Therefore, in a separate set of experiments, a second fresh chromite cylinder was introduced into the same melt from the first immersion after the first cylinder had been reacted for 4 hours. The second cylinder was then reacted for 4 hours in the same melt. A typical result is shown in Figure 4. The decrease in the carbon content of the alloy continued at almost the same rate after the immersion of the second fresh chromite cylinder, which demonstrated that artificial equilibrium existed, as a results of the formation of a product layer around the cylinders.

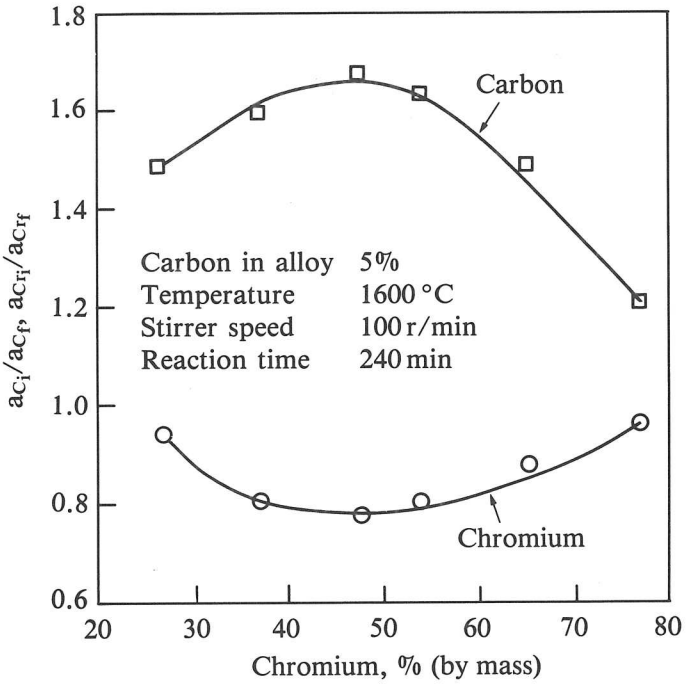

FIGURE 3. Change in initial to final activity ratios of carbon and chromium with increasing chromium content in the melt

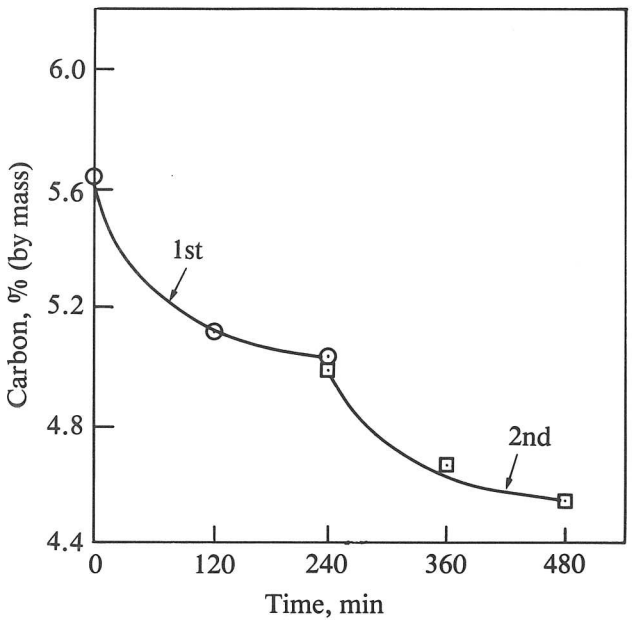

FIGURE 4. Decrease in carbon content of 50%Cr-6%C alloy as a function of time for two consecutively immersed chromite cylinders at 1600 °C, and 100 r/min

Microscopic examination of a vertical cross-section of partially reduced chromite cylinder revealed an outer metallized skin, an inner zone consisting of partially unreacted chromite, and a transition zone between the two. Microscopic examination of the outer zone under polarized light indicated the presence of a carbide phase.

In a series of experiments, chromite cylinders were individually reacted in molten 50% Cr-6% C alloys at 1600°C and 400 r/min for different times between 15 minutes and 4 hours. The phases present in the outer zone after cooling were examined by XRD. X-ray diffractograms of powdered pieces cut from the outer layer of partially reduced chromite cylinders revealed the presence of residual picrochromite, cubic $M_{23}C_6$ carbide, and hexagonal M_7C_3 carbide (M = Cr,Fe) together with α-phase (iron). For the cylinders reacted for more than 30 minutes, the diffraction pattern of the starting chromite became progressively weaker, while that of the carbides became stronger as the reaction time increased. Towards the end of the reaction period, the peaks for the α-phase and $M_{23}C_6$ also weakened and that of M_7C_3 carbide became dominant. The formation of carbides, mainly of the M_7C_3 type, around the periphery of the chromite cylinders also resulted in the retention of the original shape of the cylinder with minimal dimensional changes. At later stages of reduction, diffusion through this product layer could be the rate-controlling step.

In a subsequent experiment, a chromite cylinder was immersed in a 50% Cr- 6% C alloy at 1600°C, and liquid metallic samples were taken from the melt and quenched in water after 3 and 4 hours of reaction time. Microscopic examination of these samples revealed the presence of M_7C_3 carbide islands in the melt which contradicts the existence of a single liquid phase as indicated in the published[21-23] phase diagrams. The quenched carbides are shown in Figure 5.

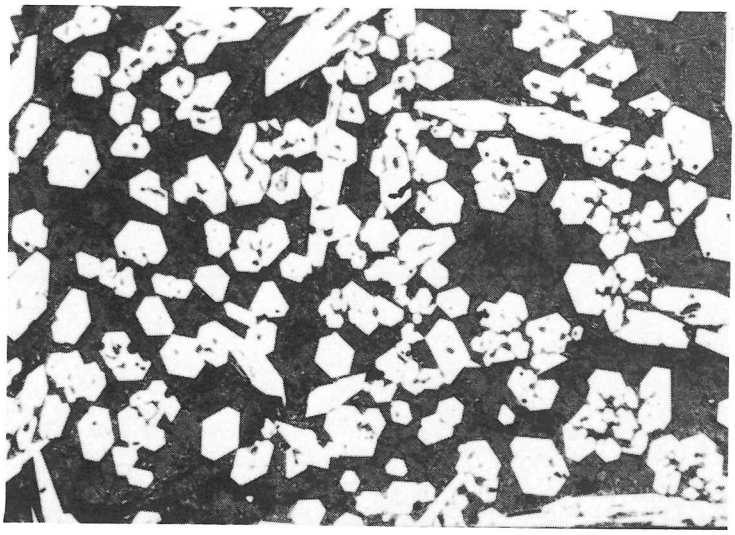

FIGURE 5. Microstructure of the 50%Cr-6%C alloy, which is reacted with the solid chromite cylinder at 1600 °C for 4 hours. The white areas are M_7C_3 carbide islands. Magnification 100×

The carbides are typically large, angular crystals of a primary phase already existing in the liquid state. It is obvious that the liquid is saturated with respect to carbide at this temperature. In the present study the Pt-6% Rh/Pt-30% Rh thermocouples used were frequently calibrated against the melting points of gold and silver, and it is estimated that the temperatures are correct to ± 5°C. It is therefore probable that there are errors in the reported liquidus surfaces.[21-23] Apparently, any carbide that forms around the periphery of the chromite cylinder will not dissolve or will dissolve very slowly in the carbide-saturated molten alloy at this temperature.

In the light of the experimental results, including microscopic examination, XRD, EMPA, and SEM-EDAX, a multistage reaction mechanism is proposed for the reduction of chromite by carbon dissolved in liquid ferrochromium alloys. In this mechanism, the Al_2O_3, MgO, and TiO_2 components of the chromite are considered unreducible. The reduction is then represented by the overall reaction (1). However, the reaction could involve the following consecutive steps:

(i) the dissociation of $FeCr_2O_4$ at the oxide-metal phase boundary

$$FeCr_2O_4(s) = 2Cr(\ell) + 4O(\%) + Fe(\ell), \quad (19)$$

(ii) transport of chromium, iron, and oxygen from the oxide-metal phase boundary to the bulk metal,

(iii) transport of oxygen and carbon from the bulk metal to the metal-gas phase boundary,

(iv) reaction of carbon and oxygen at the metal-gas phase boundary to form CO gas,

$$C(\%) + O(\%) = CO(g), \quad (20)$$

(v) and the formation of carbides with high liquidus temperatures, namely $M_{23}C_6$ and mainly M_7C_3 at the metal-oxide interface, and the transfer of carbon into the oxide through this metallized skin and/or the diffusion of carbon monoxide gas through the microcracks in this skin for further reduction. The reduction product of the chromite is now solid carbides.

It is assumed that steps (i) and (iv) are not rate determining steps because of the high temperatures involved.[24,25] Since the concentrations of chromium and iron in the liquid alloy are high and essentially constant, it is assumed that no significant chromium and iron concentration gradients exist between the boundary liquid alloy and bulk liquid alloy. Therefore, the transport of chromium and iron in step (ii) could be excluded from the rate-determining steps. The rate of reaction is affected by changes in rotational speed, particularly in the initial stage of the reduction. It is therefore presumed that the reduction is controlled by mass transfer in the melt during the initial stages. Mathematical analysis of the data confined to the liquid-state transport of carbon and oxygen species revealed that liquid-phase mass transfer of oxygen at the oxide-metal phase boundary is the most likely rate-determining step within 30 minutes of the start of the reaction. After that, reduction continues at a much slower rate by solid-state processes, resulting in the formation of carbides as the reaction product. Since the main experimental temperature was 1600°C, it could be expected that the incidence of imperfections in the spinel structure would be high, and that the assumption regarding stoichiometry of the spinel would no longer be valid. However, because of the paucity of information on the distribution and concentration of vacancies in mixed spinels, it was assumed that chrome spinel retains its stoichiometric structure with increasing reduction.

Concentration profiles for chromium, iron, aluminium, magnesium, and titanium were constructed by line scans using the SEM-EDAX facility. Three samples, one from the inner

centre zone of the particle, one from the transition zone and one from the outer metallized zone - were examined for each reduction period of between 15 minutes and 4 hours on the EDAX system. The concentration profiles for the sample from the centre zone of the particle showed no gradients, and the composition was the same as that of the original unreacted chromite. The profiles for the samples from the outer zone were typical of those for sharp phase interfaces, a metallized region enriched in iron, chromium and a chromite, but almost completely depleted in iron and relatively depleted in chromium, being observed. On the other hand, the concentration profiles for the sample from the transition zone did not show sharp phase interfaces but concentration gradients, (particularly for iron and chromium) from the inside towards the perimeter of the grains, suggesting an outward diffusion of these elements. From these profiles, cation distributions per 32 oxygens were calculated, assuming stoichiometry of the spinel as in the previous solid-state case. An example of such a calculation is given in the Appendix. However, no consistent results could be achieved with respect to the distribution of cations within the partially reduced chromite grains as a function of time. This was probably because the calculations were based on the assumption that stoichiometry holds with reduction at this high temperature.

Electron-microprobe analyses of chromite grains and the metallized regions confirmed that the metallized regions towards the interior of the cylinder consist essentially of iron. The reasons for this are quite clearly the higher reducibility of ferrous oxide, and the fact that the grains towards the interior are at an earlier stage of reduction than those at the surface. Therefore, in the early stages of reduction, metallized regions at the surface would also be rich in iron. If the diffusion of carbon through the chromite grains is negligible carbon monoxide gas can be regarded as a reductant. Figure 6 shows that metallization occurs through micro-cracks within the chromite cylinders.

Metallized regions formed at the surface of the chromite cylinder as a result of the higher degrees of reduction, are therefore richer in chromium and carbon than are the metal islands in the interior. The carbon content of the double carbide, $(Fe,Cr)_7C_3$, forming the outer metallized region was found by EMPA to be 9.3 per cent, which is in reasonable agreement with the theoretical value of 9 per cent. As further reaction occurs, metal is seen to have formed everywhere within the chromite grain. This is because, as the reduction progresses, the chromite grains exhibit a high degree of porosity, and the diffusion of carbon monoxide gas through these pores causes metallization within the grains.

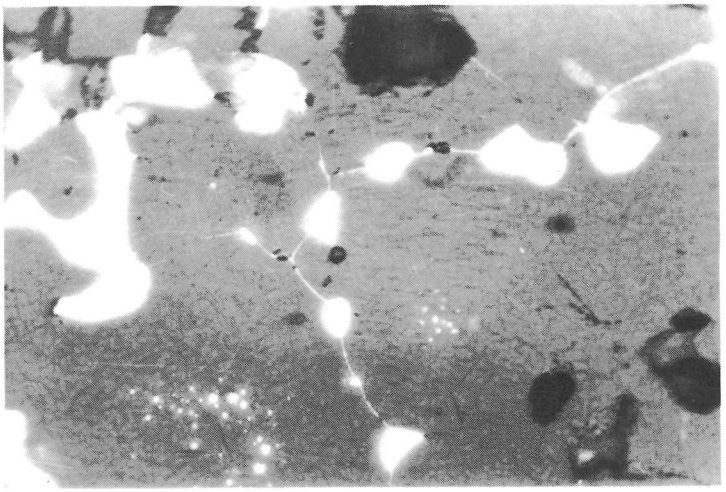

FIGURE 6. Metallization along micro-cracks within the chromite-spinel cylinder reduced in 50%Cr-6%C alloy at 1600 °C for 4 hours. Magnification 125 ×

The reaction mechanism for the reduction of LG-6 chromite at 1600°C by carbon in liquid ferrochromium alloy can be summarized as follows:

Initially, the iron oxides in the spinel reduce to form α-iron at the surface defects such as microcracks. As reduction proceeds, the reduction of iron continues, but chromium oxide also starts to be reduced. At this early stage of the reduction, oxygen transport in the liquid alloy at the oxide-melt interface is the most likely rate-determining step up to about 30 minutes of reaction time.

After the initial stage during which the melt is saturated with respect to carbide, double carbides, $(Fe,Cr)_{23}C_6$, and mainly $(Fe,Cr)_7C_3$ start to form on the surface of the chromite cylinder, thus hindering direct contact between the oxide and carbon in the liquid alloy. The reduction spreads inward from the carbide-oxide interface by a mechanism involving carbon transfer from the alloy to the chromite grains across the carbide layer. However, owing to a lack of data on the diffusion of carbon through carbides, this could not be analysed quantitatively. On the other hand, it is very likely that the diffusion of carbon monoxide gas through microcracks (and through porosities at later stages) results in further reduction and metallization on the chromite grains.

CONCLUSIONS

The study of the reduction behaviour of chromite is an ongoing research activity, which is being undertaken in an effort to understand and quantify the reduction phenomenon that covers the pre-reduction of chromite, ferrochromium smelting and refining, and stainless-steel production. The Council for Mineral Technology (MINTEK) and the University of the Witwatersrand are collaborating in this task. The results of recently completed studies and discussions reported in this paper should be interpreted on this basis. It is believed that a major advancement has been achieved in the understanding of the solid-state carbothermic reduction of chromite, the mechanistics of which are explained. This part is relevant to the pre-reduction of chromite and, to a lesser extent, to the reaction occurring in the upper parts of smelting furnaces. The dissolution of chromite into the slag phase, and the reduction from the slag, form another group of studies. On the other hand, the interaction of solid chromite directly with the metal phase is much more relevant to the refining of ferrochromium and to the making of stainless steel. Although the interaction is between the dissolved carbon of the molten alloy and the solid chromite, the process is somewhat similar to solid-state reduction. At temperatures around 1600°C, the liquid-phase processes for reduction change to what are the most probably diffusional-type solid-state processes within a fairly short time as a result of the formation of solid carbides round the chromite particles. This phenomenon is important since it leads to poor reaction rates and poor recoveries. The next step is more intensive investigation if this phenomenon and the finding of a means by which the solid-state reactions can be minimized at these smelting temperatures. The topic of this presentation was chosen to highlight these important considerations and advancements.

ACKNOWLEDGEMENTS

The author wishes to thank the Council for Mineral Technology (MINTEK) and Ferro Alloy Producers' Association of South Africa for sponsoring the work and for granting permission to publish this paper.

REFERENCES

1. G.C. Ulmer and W.B. White. "Existence of the chromous ion in the spinel solid solution series Fe Cr_2O_4-$MgCr_2O_4$". Journal of the American Ceramic Society, Vol 49, No 1, 1966, pp.50-51.

2. R.W.G. Wyckoff. "Compounds of the type R_2MX_4". Crystal Structures, Interscience Publishers, New York, N.Y., 1965, pp.77-82.

3. K.P.D. Perry. "Thermodynamical analysis of the reduction of chromites", PhD Thesis, University of the Witwatersrand, Johannesburg, 1986.

4. F.A. Kroger. "Imperfection equilibria in pure binary compounds". The Chemistry of Imperfect Crystals, Vol.2,(2nd ed) American Elsevier, New York, N.Y., 1974, pp.237-339.

5. G. Castle and P.L. Surman. "The self diffusion of oxygen in magnetite". Journal of Phys. Chem., Vol.71, 1967, pp.4255-4259.

6. E.J.M. Verwey. Z. Kristallog, Vol.91, 1935, pp.65-71.

7. R. Dieckmann and H. Scmalzried, "Defect and cation diffusion in magnetite". Berigte Busenges der Phys. und Chem., Vol.8, No.4, 1977, pp.414-419.

8. C.S. Kucukkaragöz, S.H. Algie and C.W.P. Finn. "The reduction of Winterveld chrome spinel at 1300°C and under an argon atmosphere in the presence of carbon". Report M 154, Council for Mineral Technology, Randburg, 1984.

9. W.J. Rankin. "The composition and structure of chromite during reduction with carbon". Arc. Eisenhuttenwes, Vol.50, No.9, 1979, pp.373-378.

10. E.D. Kinloch. "The role of mineralogy in pilot plant prereduction of chromite ores in South Africa". Proceedings of 1st Int. Congress on Appl. Mineral.. Geol. Soc. of Southern Africa, Johannesburg, 1983, No.7,pp.337-349.

11. M.J. Searle and C.W.P. Finn. "Mathematical modelling of the reduction behaviour of chromite from the upper chromite layer of the Bushveld Complex", Report M 96, Council for Mineral Technology, Randburg, 1983.

12. C. Greskovich and V.S. Stubican. "Divalent chromium in magnesium-chromium spinels" Journal of Phys. Chem. of Solids, Vol.27, 1966, pp.1379-1384.

13. A. Novakova, C. Kleir and K.S. Jiru. "Exchange reactions between solid oxides and oxygen molecules", Reactivity of Solids, Elsevier, New York, N.Y., 1965, pp.269-278.

14. O. Katsutoshi and S. Awazu. "Oxygen penetration into $CaF_2:Sm^{2+}$ crystals". Journal of Phys. Chem. of Solids, Vol.29, 1968, pp.1269-1273.

15. S.A. De Waal and S.A. Hiemstra, "The mineralogy, chemistry, and certain aspects of reactivity of chromitite from the Bushveld Igneous Complex". Report 1709, National Institute for Metallurgy, Johannesburg, 1975.

16. A Navrotsky and O.J. Kleppa. "The thermodynamics of cation distribution in simple spinels". Journal of Inor, Nucl. Chem., Vol.29, 1976, pp.2701-2714.

17. J.O. Edstrom. "The mechanism of reduction of iron oxides", Journal of Iron and Steel Inst., Vol.175, 1953, pp.289-304.

18. J.O. Edstrom. Jernkont. Ann. 191, Vol.12, 1957, pp.809-813.

19. L.N. Barmin et al. "Kinetics of reduction of solid Cr(III) by carbon dissolved in Fe", Izv. VUZ Chemica Metallurgiya, Vol.11, No.8, 1968, pp.20-23.

20. G.W. Healy. "Activities in the liquid Cr-Fe-C system above 1600°C". Proceedings of the Reinhard Schuhmann International Symposium on Innovative Techology and Reactor Design in Extractive Metallurgy", Colorado Springs, CO., 1986, pp.667-679.

21. N.R. Griffing, W.D. Forgeng and G.W. Healy. "C-Cr-Fe liquidus surface". Trans, Metall. Soc. AIME, Vol.224, 1962, pp.148-159.

22. R.S. Jackson. "The austenite liquidus surface and the constitutional diagram for the Fe-Cr-C metastable system". J.I.S.I., Vol.208, No.2, 1970, pp.163-167.

23. J.C.M. Wethmar. "Phase equilibrium in the Cr-Fe-Si-C system in the composition range representative of high carbon ferrochromium alloys produced in South Africa". Report 1457, National Institute for Metallurgy, Johannesburg, 1972.

24. R.J. Fruehan. "Rate of reduction of Cr_2O_3 by carbon and carbon dissolved in liquid iron alloys". Metall. Trans. Vol.8B, 1977, pp.429-433.

25. P. Sjoval. Proceedings of the Second Japan-Sweden Joint Symposium on Ferrous Metallurgy Iron and Steel Institute of Japan, Tokyo, 1978, pp.74.

26. O. Soykan. "The Solid State Reduction Characteristics of the Bushveld Complex Chromites", Ph.D. Thesis, University of the Witwatersrand, Johannesburg, 1988.

APPENDIX

AN EXAMPLE OF THE CALCULATION OF CATIONS/32 OXYGENS FROM EDAX ANALYSIS.

The sample is an unreduced chromite particle. The mass percentages from EDAX are converted into atomic fraction as follows:

Element	Mg	Al	Ti	Cr	Fe	O
Mass %	5.66	7.52	0.44	32.90	20.06	30.81
N_i	0.07	0.08	0.003	0.18	0.10	0.56

The number of cations per 32 oxygens are calculated as follows:

		Norm to 24	
$\frac{N_{Mg}}{N_O} \times 32$	= 4.00		4.00 x $\frac{24.0}{24.72}$ = 3.88
$\frac{N_{Al}}{N_O} \times 32$	= 4.57		= 4.44
$\frac{N_{Ti}}{N_O} \times 32$	= 0.15		= 0.15
$\frac{N_{Cr}}{N_O} \times 32$	= 10.29		= 9.99
$\frac{N_{Fe}}{N_O} \times 32$	= 9.71		= 5.54
Total	24.72		24.00

Normalization to 24 is necessary since it is assumed that 8 tetrahedral and 16 octahedral sites are occupied by cations. Since Ti^{4+} makes ulvospinel with Fe^{2+} in the octahedral sites, the distribution of cations will be as follows.

Fe^{2+} in octahedral sites = 0.15
Fe^{3+} in octahedral sites =[(5.54-0.15)+3.88]-8
=1.27
Fe^{2+} in tetrahedral sites=5.54-0.15-1.27 =4.12
Mg^{2+} in tratrahedral sites = 3.88

Cr^{3+} in octahedral sites = 9.99
Al^{3+} in octahedral sites = 4.44

Consequently, for this particular EDAX analysis, the chemical formula for unreduced chromite is

$$(Fe_{4.12}^{Mg}{}_{3.88})[Cr_{9.99}Al_{4.44}Fe^{3+}_{1.27}Fe^{2+}_{0.15}Ti_{0.15}]O_{32}$$